



Facies Associations of Early Cretaceous Arumit Formation and Early to Late Cretaceous Ungar Formation in Vulmali and Ungar Islands, Tanimbar (Indonesia)

RAKHMAT FAKHRUDDIN

Centre for Geological Survey, Geological Agency, Ministry of Energy and Mineral Resources
Jln. Diponegoro No.57 Bandung, Jawa Barat, Indonesia

Corresponding author: rakhmat.fakhruddin@esdm.go.id
Manuscript received: June, 29, 2018; revised: August, 27, 2018;
approved: April, 20, 2019; available online: July, 30, 2019

Abstract - Cretaceous sediments are among the important petroleum system elements for hydrocarbon exploration in Tanimbar area. However, little is known about their facies associations and depositional environments. Facies association analyses have been carried out in fourteen surface sections. Early Cretaceous Arumit Formation comprises three facies associations: subtidal, intertidal, and supratidal deposits. A progradational open-coast tidal flat depositional environment suggests the deposition of sediments of the Arumit Formation. The presence of tidal rhythmites, mud drapes, and fluid mud in those sediments are diagnostic features of a tide domination process in deposition of this unit. Early to Late Cretaceous Ungar Formation in the studied area consists of four facies associations: intertidal, marine offshore to lower shoreface, upper shoreface, and foreshore deposits. An open-coast wave dominated depositional environment is proposed for deposition of sediments of the Ungar Formation. Wave dominated environments in the coarsening upward interval is represented by hummocky cross stratification, cross-bedded sand and gravel, planar parallel stratification, and low-angle stratified beds.

Keywords: Cretaceous, Tanimbar, Arumit Formation, Ungar Formation

© IJOG - 2019. All right reserved

How to cite this article:

Fakhruddin, R., 2019. Facies Associations of Early Cretaceous Arumit Formation and Early to Late Cretaceous Ungar Formation in Vulmali and Ungar Islands, Tanimbar (Indonesia). *Indonesian Journal on Geoscience*, 6 (2), p.185-208. DOI: [10.17014/ijog.6.2.185-208](https://doi.org/10.17014/ijog.6.2.185-208)

INTRODUCTION

Cretaceous sediments exposed in the studied area are thought to be age equivalent to the Echuca Shoals petroleum system in the northern Bonaparte Basin (Barber *et al.*, 2003). The elements of this hypothetical petroleum system involve Early Cretaceous source rocks and Late Cretaceous reservoirs. The Cretaceous sediments in the Tanimbar Islands are known as Ungar Formation (Kaye, 1989; Charlton *et al.*, 1991),

which is previously included in the Molu Complex (Sukardi and Sutrisno, 1989).

Ungar Formation consists of two distinct members (Charlton *et al.*, 1991). First, orange or yellow weathering massive to poorly bedded, very coarse (up to 3 - 4 mm) mature quartz sandstones, composed of well-rounded and moderately to well sorted quartz grains, with a minor clay matrix sometimes present. Second, greenish or buff fine-medium arkosic sandstones comprising angular to rounded grains, with a glauconite and

clay matrix. The first sandstone member occurs in Vulmali Island, and in the ejecta of some mud volcanoes, while the second sandstone member outcrops in Ungar and Natraal Islands. A possible fluvio-deltaic environment of deposition suggested for depositional environment of the Ungar Formation (Charlton, 1991), probably in a high energy shoreface with massive channeled and clean sandstone (Kaye, 1989).

A sequence of mudrock and radiolarian silts is included in Ungar Formation, or possibly at its base, named informally as the Arumit Member of the Ungar Formation (Charlton, *in* Jasin and Haile, 1996). The radiolarian chert interbedded with sandstones and shales outcropping in the west of Ungar Island is the much rarer chert *in situ* type deposited in a deep water environment (even bathyal) adjacent to a land area (Jasin and Haile, 1996). While depositional environment interpretation for radiolarian silts and muds of the Arumit Member was a low energy and restricted shallow marine setting (Kaye, 1989).

Furthermore, the Ungar Formation is divided into upper part and lower part (Charlton, 2012). The upper part is a major sandstone unit, which interdigitates with radiolarian shales (Arumit Member). This unit is dated as Early Cretaceous, Berriasian-Barremian age (Jasin and Haile, 1996), while by a shale sample from a mud volcano it has been dated as Hauterivian (Charlton, 2012). The lower part of the Ungar sandstones underlying the Early Cretaceous radiolarian shales is likely to be Late Jurassic in age (Charlton, 2012).

Ungar Formation is categorized into Jurassic Ungar Formation and Cretaceous Ungar Formation (Zimmermann and Hall, 2014). They described Jurassic Ungar Formation as comprising immature massive greyish brown sandstones (quartz arenite, sublithic arenite, subfeldspathic arenite) with fine- to medium- grain size. While Cretaceous Ungar Formation is massive white-beige to yellowish fine- to coarse-grained sandstones (quartz arenite, subfeldspathic arenite, arkosic arenite). Zircon U-Pb ages for the Jurassic Ungar Formation, the youngest grain are Lower Jurassic, 195.7 Ma, while for the Cretaceous

Ungar Formation, the youngest grain is Late Cretaceous, 83.7 Ma (Zimmermann and Hall, 2014).

However, little is known about facies associations and depositional environments of Arumit and Ungar Formations. This paper is intended to describe the facies association and depositional model of Arumit and Ungar Formations outcropping in Vulmali and Ungar Islands, Tanimbar. The results of this paper are expected to provide some preliminary information on the exploration of new hydrocarbon resources in Tanimbar Island region and surrounding areas and to scholars engaged in researching Mesozoic palaeogeographic reconstructions of southeastern Asia.

Geological Setting

The Tanimbar Islands are located in the southeastern part of the Banda arc-continent collision zone which structurally comprise a fold and thrust belt (Charlton, 2018). Stratigraphic information of Tanimbar Islands is inferred from limited rock exposure and mud volcano ejecta (Charlton, 2012). The Permian to Early Cretaceous stratigraphic succession was deposited within, and on the western flank of a large graben setting (the Tanimbar Graben) which probably began to develop during the Permian as an aulacogenic rift on the northern margin of the South Banda Graben as the northward continuation of the Calder Graben on the Australian continental margin (Charlton, 2012, 2018).

The oldest rocks on Tanimbar are of Permian age, shallow marine carbonate and volcanic successions of Selu Formation (Charlton, 2012, 2018). During Middle Triassic to Early Jurassic, a fluviodeltaic succession (Maru Formation) and restricted marine carbonate successions (Wotar Formation) were deposited in the Tanimbar Graben (Charlton *et al.*, 1991; Charlton, 2018). The Maru and Wotar Formations are succeeded by Early to Middle Jurassic transgressive shales which are interpreted to be deposited in a low-energy restricted marine environment (Charlton *et al.*, 1991; Charlton, 2012, 2018). The Late Jurassic to Early Cretaceous sediments of the Tanimbar Graben are represented by the studied

units, the Ungar Formation and Arumit Member (Charlton *et al.*, 1991; Charlton, 2018). The Late Cretaceous to Paleogene succession is a deep-water carbonates sequence that was deposited on the Australian margin after continental breakup (Charlton *et al.*, 1991; Charlton, 2012, 2018).

METHOD

Detailed sedimentological observations were performed at sedimentary successions outcropping along the foreshore of Vulmali and Ungar Islands, Tanimbar (Figure 1), to develop facies for constraining probable depositional environments. Observations of the sediments were primarily focused on features such as colour, textures, grain sizes, bed thicknesses, sedimentary structures, bed

contacts, and stratigraphic relationships. The total of fourteen detailed sedimentary logs was produced, divided into three stratigraphic intervals. First, eleven sedimentary logs (MS 1-MS 11) at the west coast of Vulmali Island (west Vulmali section, Figure 2). MS 1-MS 11 are considered as one stratigraphic interval based on their stratigraphic position relatively similar dipping to northward. The thickness of non-exposure rocks in this section was calculated by GPS waypoints combined with the average of dip measurements. Second, two sedimentary logs (MS 12 and MS 13) at the west coast of Ungar Island (west Ungar section, Figure 3). Third, one sedimentary log (MS 14) is at the east coast of Vulmali Island (east Vulmali section, Figure 4). Facies associations corresponding to groups of facies are genetically related to one another and have some environmental significance

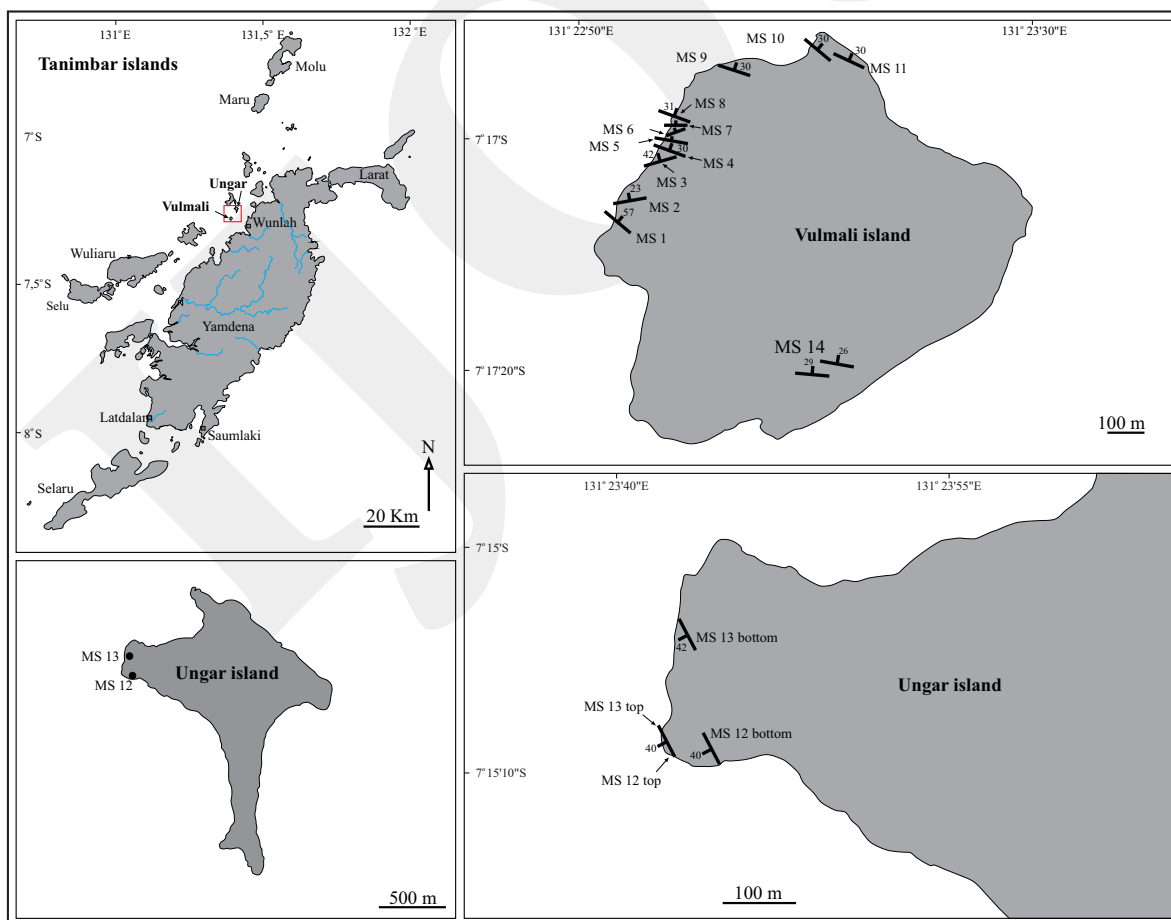


Figure 1. Location map of the studied areas at the Vulmali and Ungar Islands, Tanimbar Islands, showing the position of outcrop measured sections: west Vulmali section (MS 1–MS 11), west Ungar section (MS 12 and MS 13), and east Vulmali section (MS 14).

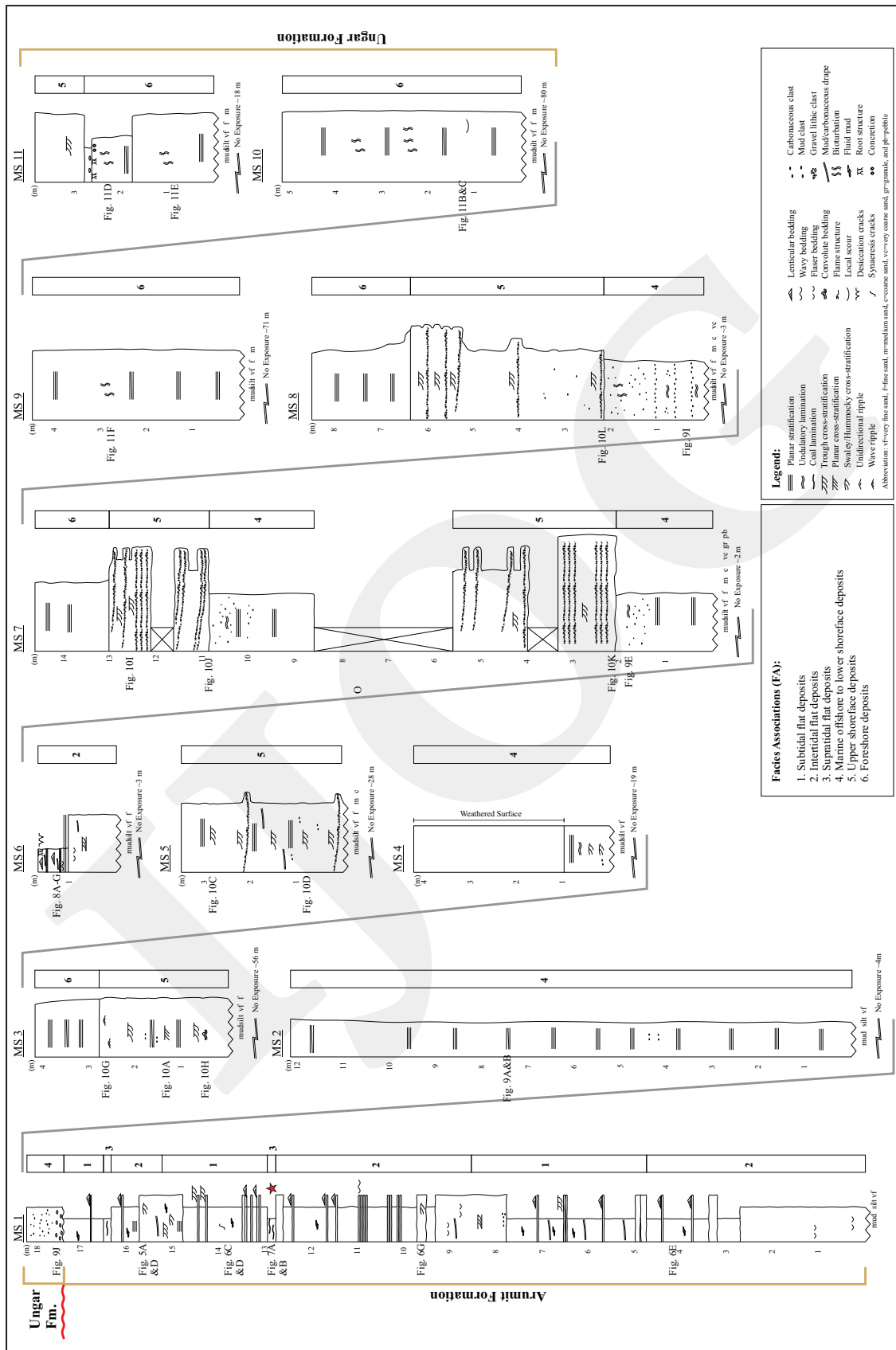


Figure 2. Composite sedimentary log of west Vulmali section. Red star indicate the position of palynological sample of lignite layer of the Arumit Formation.

Facies Associations of Early Cretaceous Arumit Formation and Early to Late Cretaceous Ungar Formation in Vulmali and Ungar Islands, Tanimbar (Indonesia) (R. Fakhruddin)

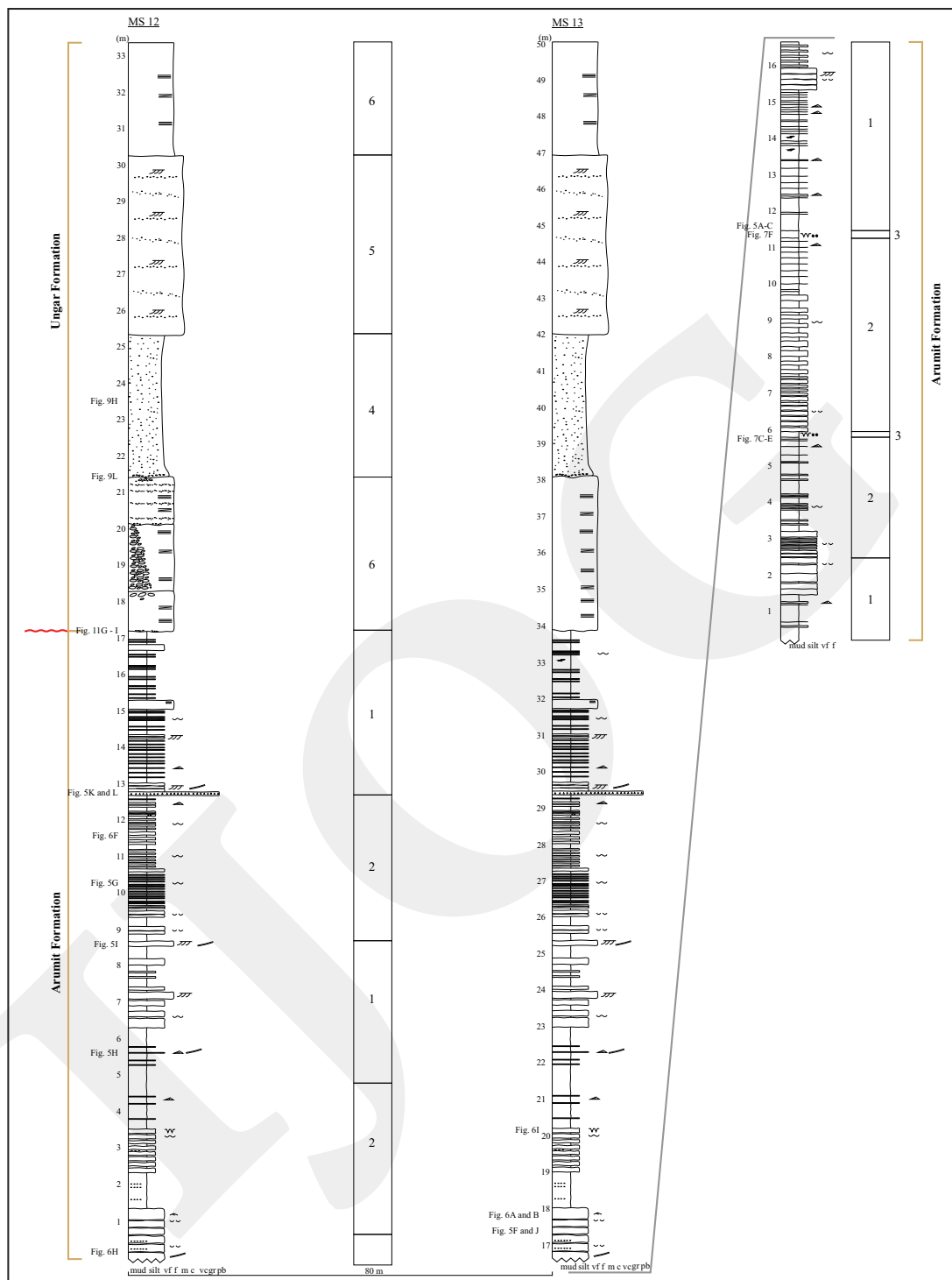


Figure 3. Composite sedimentary log of west Ungar section. Legend: see Figure 2.

(Collinson, 1969, *in* Walker, 2006), as subenvironments within a depositional system. The facies associations were classified based on similarity of sedimentary features, following a classifications based on Clifton (2006) and Fan (2013).

Palynological analysis for the purpose of age determination was carried out in GeolLabs, Pusat Survei Geologi. Ten samples (9 mudstones and 1 lignite of Arumit Formation) were prepared for the palynological analysis. Palyno-

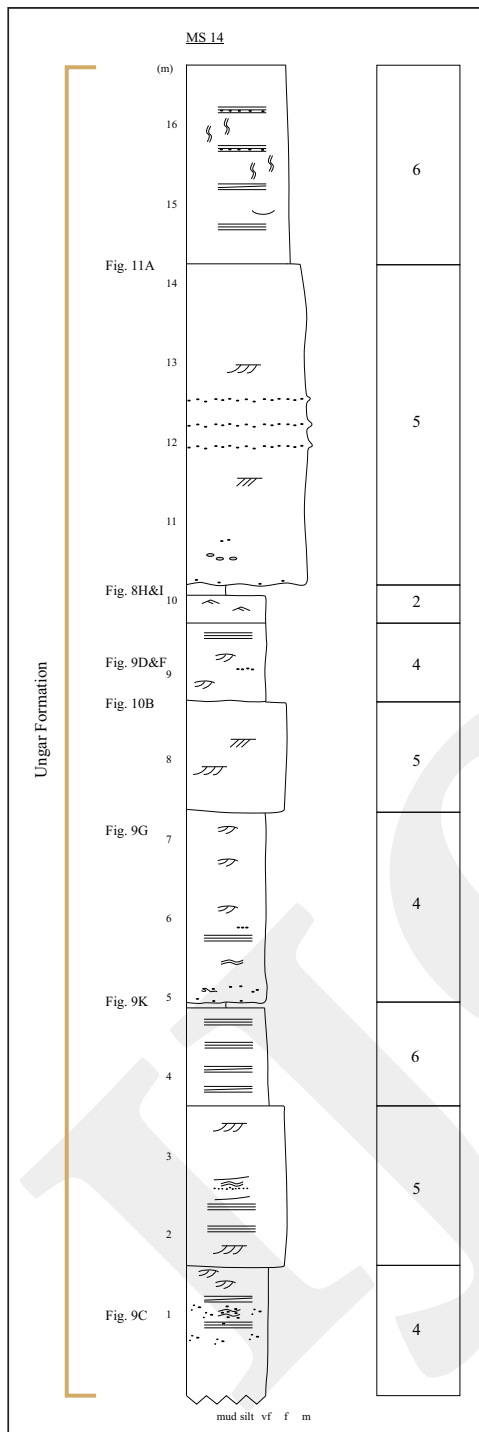


Figure 4. Composite sedimentary log of east Vulmali section. Legend: see Figure 2.

morph analysis involved extraction from 100 gr samples was carried out using HF and HCl. Palynomorphs were separated from the substrate using zinc chloride solution. The residue was then sieved with a 5 µm mesh and mounted on slides with glycerin jelly. Palynomorph obser-

vation was done using a 1000X magnification polarization microscope.

RESULTS and DISCUSSIONS

Sedimentary logs from Arumit and Ungar Formations are shown in Figures 2, 3, and 4. Moreover, selected outcrop and facies shots are shown in Figures 5 to 11. Facies observations from Arumit Formation show the domination of heterolithic bedding consisting of mudstone to siltstone alternating with very fine- to fine-grained sandstone (Facies association 1 and 2) to a mudstone to silty mudstone with lignite laminae (Facies association 3) (Figure 2 and 3). Facies observations from Ungar Formation generally indicate coarsening upward successions from very fine-grained sandstones in the basal portion (Facies association 4), through fine- to medium-grained sandstones, with layers and lenses of granule sandstones and granule to pebble conglomerates in the middle portion (Facies association 5) to very fine- to medium-grained sandstones (Facies association 6) in the upper portion (Figure 2, 3, and 4). Uncommon fine-grained sandstone-dominated to mudstone-dominated facies of Ungar Formation (Facies association 2) occurs at west Vulmali section (Figure 2). Rare matrix mud supported and lithic clast facies with the clast size up to boulder size were found at MS 12 of west Ungar section (Figure 3). The erosional contact between the two formations is found at MS 1 of west Vulmali section (Figure 2) and at MS 12 and MS 13 of west Ungar section (Figure 3).

Arumit Formation

Facies association 1 (FA1): subtidal flat deposits

Description

Arumit Formation subtidal facies association is dominated by heterolithic bedding consisting of red, brown to dark brown mudstone to siltstone alternating with thin beds of reddish brown to greenish gray very fine- to fine-grained sandstone (Figures 2, 3, and 5). Mudstone and sandstone layers alternatively dominate in dif-



Figure 5. Field photographs of subtidal flat deposits (FA1) of Arumit Formation. Height of the man is 170 cm. Diameter of the coin, length of hammer and pen is 2.7 cm, 33 cm and 14.5 cm respectively. a, b, and c) FA1 heterolithic bedding of mudstone to siltstone alternating with thin beds of very fine- to fine-grained sandstone showing coarsening upward succession. White line: FA boundary. d and e) Millimeter thick tidal rhythmites showing possible neap (n) and spring (s) tidal cycles, single and double mud drapes (white arrows), hummocky (yellow arrows) and swaley cross-stratification (orange arrows). f) Flaser bedding showing mudstone lenses (red arrows) within predominant very fine-grained sandstone. Below the hammer is double carbonaceous drapes in planar lamination (white arrows). g) Wavy bedding showing alternation of very fine sandstone with mudstone. h) Lenticular bedding showing current rippled sandstone (red arrow) within mudstone, with mud and carbonaceous drape (white arrows). i) Possible tidal bundle showing cross-laminated fine-grained sandstone with mud draped foresets (white arrow). j) Planar laminated silty mudstone with organic debris. Some laminae contain single and double carbonaceous drapes (white arrows). k and l) Cross-bedded silty very fine-grained sandstone with mud drape (white arrow) separates the cross-bed into tidal bundles. Pebble sized mud clasts layer (red arrows) occurring at the base of the cross-bedded sand.

ferent sets, with the thickness ranging from 1 mm to few centimetres, sometimes making up millimeter to centimeter thick tidal rhythmites (Figure 5). The thickness of facies association is up to 5.5 m thick. The main feature is coarsening

upward successions with regular changes vertically from lenticular bedding, through wavy bedding, and to flaser bedding. Cross-bedded and cross-lamination sand is locally present in this FA with mud drapes in a cross-bed/laminae that

separates the cross-bed/laminae into tidal bundles (Figures 5i, k and l). Pebble sized mud clast layer locally occurs at the base of cross-bedded sand (Figures 5k and l). Single and double mud drapes locally occur in this FA both in planar and cross-laminated beds (Figures 5d, e, i, k, and l). Organic debris occurs rarely, present as single and double carbonaceous drapes marking stratification (Figures 5f and j). Sandstone layers contain current ripple (Figures 5h, 6a and b), planar lamination (Figures 5d - f and j), hummocky, and swaley cross-stratification (Figures 5d and e). Fluid mud found in this association is light green in colour, occurring as fluid mud layers (Figures 6c and d) and rip up clasts with

the layer thickness from < 1 to 15 cm (Figure 6e). Light green fluid mud also occurred filling cracks (Figures 6c and d).

Interpretation

Heterolithic character indicates repeated fluctuations in the energy regime, with both sand and mud available (Boyd *et al.*, 2006; Davis, 2012). Gradational spectrum of heterolithic deposits with alternating beds/laminae of sand and mud produces lenticular, wavy, and flaser bedding (Fan, 2013). Heterolithic bedding with lenticular, wavy, and flaser bedding primary occurrence is in tidal settings (Reineck and Singh, 1980; Dalrymple, 2010), but they may

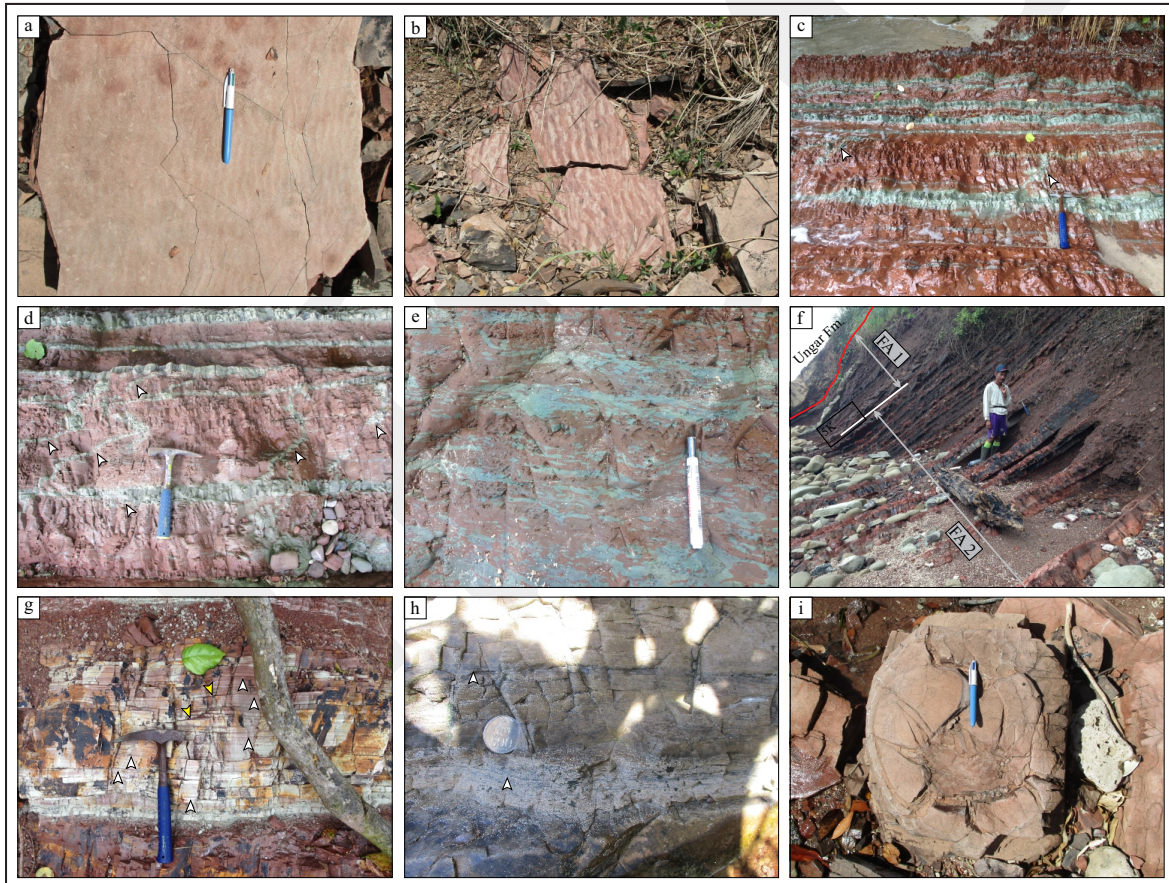


Figure 6. Field photographs of subtidal flat deposits (FA1) (a - e) and intertidal flat deposits (FA2) of Arumit Formation (f - i). Height of the man is 170 cm. Length of the pen, hammer, marker, and diameter of coin is 14.5 cm, 33 cm, 14.5 cm and 2.7 cm respectively. a and b) Current ripple mark on bedding plane of very fine-grained sandstone. c and d) Fluid mud layer (light green colour) alternating with mudstone (red colour) showing fluid mud filling synaeresis cracks (white arrows). e) Mudstone bed contain fluid mud rip up clasts. f) Heterolithic bedding of mudstone to siltstone alternating with thin beds of very fine- to fine-grained sandstone showing FA2 fining upward succession. White line: FA boundary, red line: unconformity/formation boundary. g) Rhythmic lamination showing probable tidal cycle which contain mud drapes (white arrows) and hummocky cross-stratification (yellow arrows). h) Carbonaceous drape parallel laminae (white arrow) and organic debris intercalation with silty mudstone and very fine-grained sandstone. i) Desiccation cracks in the siltstone of FA2.

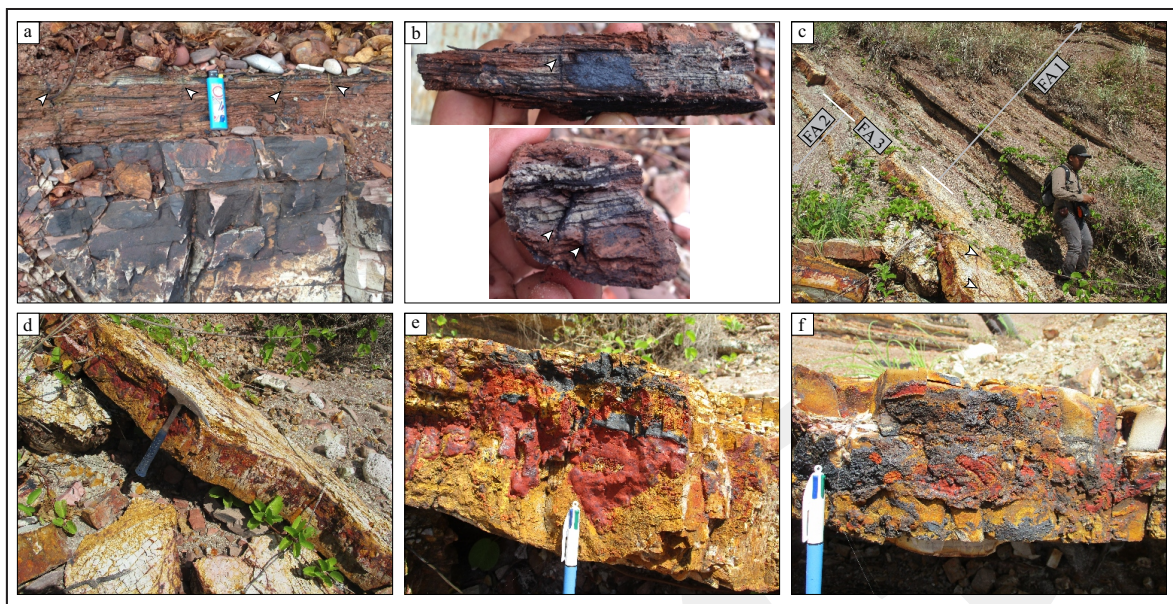


Figure 7. Field photographs of supratidal flat deposits (FA3) of Arumit Formation. Height of the man is 170 cm. Length of the lighter, hammer and white portion of the pen is 8 cm, 33 cm and 6 cm respectively. a) Alternation of mudstone bed to silty mudstone laminae with discontinuous lignite laminae showing root structure (white arrows). b) Rhythmic alternation of lignite laminae with silty mudstone showing root structure (white arrows). c - f) White cream-coloured mudstone, undulatory surface with red, black and orange Fe-mineralization fill in the cracks. Incomplete desiccation mudcrack structure showing triple junctions (white arrows). White line: FA boundary.

also be formed by episodic flooding on the alluvial plains, or weak storms in the offshore environments (Fan, 2013). Sand is formed from current or wave activity, while mud is deposited during suspension (Reineck and Singh, 1980). Tidal bedding regular changes from lenticular bedding, flaser bedding through wavy bedding of this FA are interpreted to form in a subtidal setting (Fan, 2013).

Tidal rhythmites consist of cyclical stacking of horizontal laminations or beddings bearing neap-spring cyclicity whose thickness varies rhythmically (Dalrymple, 2010; Longhitano *et al.*, 2012; Fan, 2013). Thick sandy beds/laminae represent a deposition of spring tides, while thin sandy layer beds/laminae are products of neap tides, and spring-neap cycles caused by their regular alternations (Fan, 2013). Heterolithic cycle thickness and the number of laminae indicate tidal periodicities of short duration (from semidiurnal, neap-spring to monthly) to longer tidal cycles (up to annual) (Longhitano *et al.*, 2012). Alternations of sandier and muddier packages as centimeter bedding in this FA are probably related to longer tidal cycle.

Dune migration in the subtidal part of tidal channels produces cross-bedded sands (Ashley, 1990; Choi *et al.*, 2004). Heterolithic facies above cross-bedded sands reflect a gradual decrease in the current speed from the deeper parts of the channel to the channel bank (Mossop and Flach, 1983). The presence of mud drapes which separates the cross-bed into tidal bundles suggests slack water periods during a high or low tide (Dalrymple and Choi, 2007; Longhitano *et al.*, 2012). Poorly rounded and moderately sorted mud clasts below the tidal bundle show relatively low maturity of textures of these deposits which indicate transportation in a limited distance of reworked unconsolidated muddy sediments by tides (Li *et al.*, 2017). The presence of this mud clast layer below tidal bundles suggests they were developed at tidal channel base deposits (Dalrymple and Choi, 2007).

Mud/carbonaceous drapes formed during the slack-water periods within cross-beds and/or between sets of ripple cross-lamination (Dalrymple and Choi, 2007; Longhitano *et al.*, 2012), and also formed in the planar laminated beds

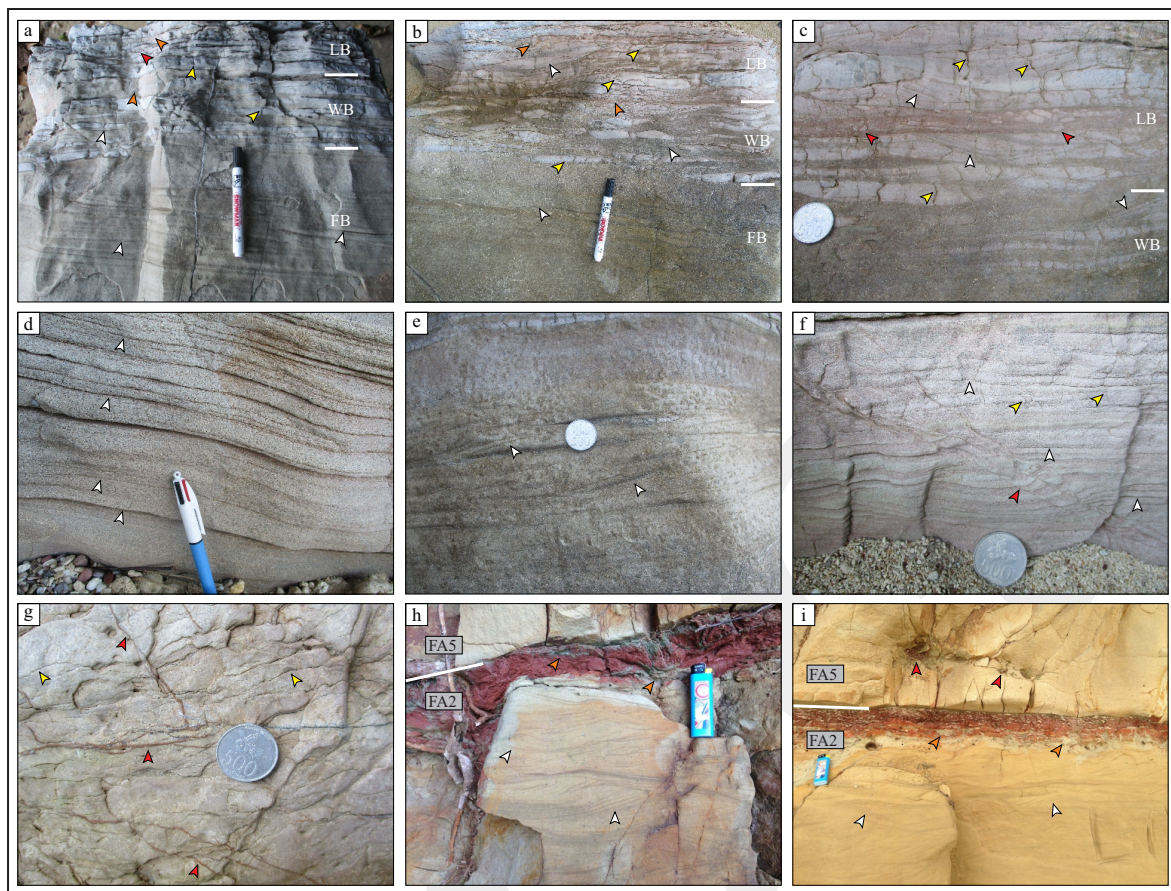


Figure 8. Field photographs of intertidal flat deposits (FA2) of Ungar Formation. Length of the marker, white portion of the pen, lighter, and diameter of coin is 14.5 cm, 6 cm, 8 cm and 2.7 cm respectively. Abbreviation = LB: lenticular bedding, WB: wavy bedding and FB: flaser bedding. a - c) Vertical changes from flaser bedding, through wavy bedding, and to lenticular bedding in a fining upward succession of dominant fine-grained sandstones at the lower part to dominant mudstone at the upper part. Single and double mud/carbonaceous drapes (white arrows) present in all interval. Cross-beds occur in fine-grained sandstones (flaser bedding interval) with mud drapes separates the cross-bed into tidal bundles. Numerous desiccation cracks are present predominantly in the mudstone (yellow arrows). Root structures (red arrows) and mudstone intraclasts (orange arrows) occur in the lenticular bedding interval. d and e) Rhythmic alternation of mud drapes (white arrows) and sandstone in the cross-bed forming tidal bundle. f) Rhythmic alternation of mudstone, mud drapes (white arrows) and sandstone in the planar laminae. Note the presence of minor syndimentary fault (red arrow) and desiccation cracks (yellow arrows). g) Root structure (red arrows) and desiccation cracks (yellow arrows) in bedding plane of mudstone dominated interval. h and i) Current ripple sandstone with mud draped foresets (white arrows) overlain by red mudstone which contain fluid mud (orange arrows). White line: FA boundary. Note the erosional contact between FA2 and FA5 above it and the presence of mudclasts (red arrows) above the contact.

(Vakarelov *et al.*, 2012). The mud drapes may be single or double, depending on whether there are one or two slack-water periods (Dalrymple and Choi, 2007). The occurrence of current ripple cross-lamination supports the presence of tides. Typical storm-generated thin layers of micro HCS and SCS indicate storm influence in the setting (Vakarelov *et al.*, 2012; Fan, 2013).

Fluid mud is any aqueous suspension in which the mud concentration of particles is > 10 gr/l (Kirby and Parker, 1983; Faas, 1991). In a tidal

setting, fluid mud forms below a turbidity maximum zone, a zone of elevated suspended sediment (Dalrymple and Choi, 2007; Ichaso and Dalrymple, 2009; Longhitano *et al.* 2012). The fluid mud layers are products of slack water within a single tidal cycle (Dalrymple and Choi, 2007; Longhitano *et al.* 2012), and are also able to form during storms when wave energy is high (Ichaso and Dalrymple, 2009). Ripped-up clasts of fluid mud were interpreted as a penecontemporaneous erosion of fluid mud layer. Fluid mud filling cracks are interpreted as syaere-

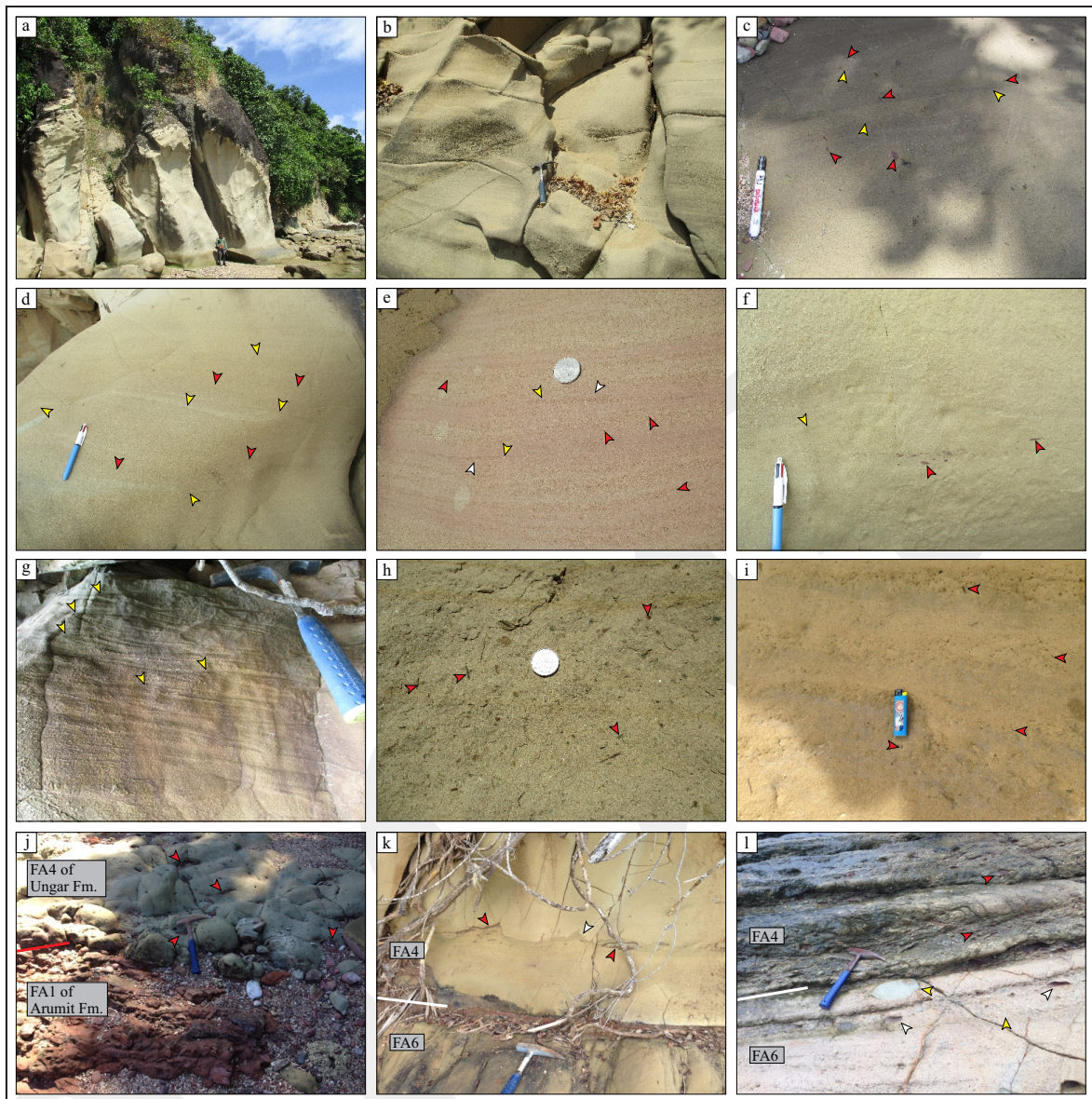


Figure 9. Field photographs of marine offshore to lower shoreface deposits (FA4) of Ungar Formation. Height of the man is 170 cm. Length of the hammer, marker, pen, lighter and diameter of coin is 33 cm, 14.5 cm, 14.5 cm, 8 cm and 2.7 cm respectively. a and b) Parallel laminated to low-angle laminated very fine-grained sandstones with sharp base. c) Carbonaceous detritus concentration (yellow arrows) in the undulatory lamination with scattered granule to pebble clasts (red arrows). d - g) Hummocky cross-stratification (yellow arrows) with scours likely related to storm-generated currents and the presence of scattered granule to pebble clasts (red arrows) probably related to post-storm event. Carbonaceous detritus concentration (white arrows) present in the undulatory lamination. h and i) Numerous scattered granule to pebble clasts (red arrows) in the sandstone of FA4. j) Erosional contact between FA1 of Arumit Formation and FA4 of Ungar Formation show mud clasts (red arrows) above the contact. Red line: unconformity/formation boundary. k and l) Erosional contact between FA6 and FA4 with mud clasts (red arrows) and flame structure (white arrow) above the contact. FA6 consist of mud (white arrows) and lithic (yellow arrows) clasts in fine-grained sandstone. The clasts are present in scattered and layered forms. White line: FA boundary.

sis cracks filling which infilled the less dense mud in which they grow. Subaqueous syneresis cracks are formed in mud by the spontaneous dewatering of clay beneath a body of water (White, 1961; Plummer and Gostin, 1981).

Facies association 2 (FA2): Intertidal flat deposits *Description*

Arumit Formation intertidal facies association is dominated by heterolithic bedding of red, brown to dark brown mudstones to siltstones



Figure 10. Field photographs of upper shoreface deposits (FA5) of Ungar Formation. Length of the pen, hammer and marker is 14.5 cm, 33 cm and 14.5 cm respectively. a) Succession of planar bedding, planar cross-bedding and low-angle cross-bedding fine-grained sandstone. b) Planar bedding and planar cross-bedding fine-grained sandstone (FA5) is overlain by erosional contact with undulatory lamination and hummocky cross-stratification of very fine-grained sandstone of FA4. White line: FA boundary. c - f) Trough cross-bedding medium- to coarse-grained sandstone. g) Wave ripple fine-grained sandstone. h). Convolute bedding overlain by low-angle cross-bedding fine-grained sandstone. i - k) Cross-bedded sand and granule to pebble. Figure j and k show erosional contact between FA4 and FA5. White line: FA boundary. l) Transition from lower shoreface (FA4) to upper shoreface (FA5). Lower shoreface has scattered granule to pebble in sandstone. Upper shoreface marked by cross-bedded sand and granule to pebble. White dash line: FA boundary.

alternating with thin beds of reddish brown to greenish gray very fine- to fine-grained sandstone (Figures 2, 3, and 6f-i). Mudstone and sandstone layers range from 1 mm to few centimeters, while facies association units are up to 5.3 m thick. Millimeter to centimeter thick cyclical tidal rhythmites are observed (Figure 6g). The main

feature of this FA is fining upward successions with regular changes vertically from flaser bedding, through wavy bedding, and to lenticular bedding (Figure 6f). Single and double mud/ carbonaceous drapes are uncommon as well as organic debris clasts layered in the planar laminated beds (Figure 6h). Rare desiccation cracks

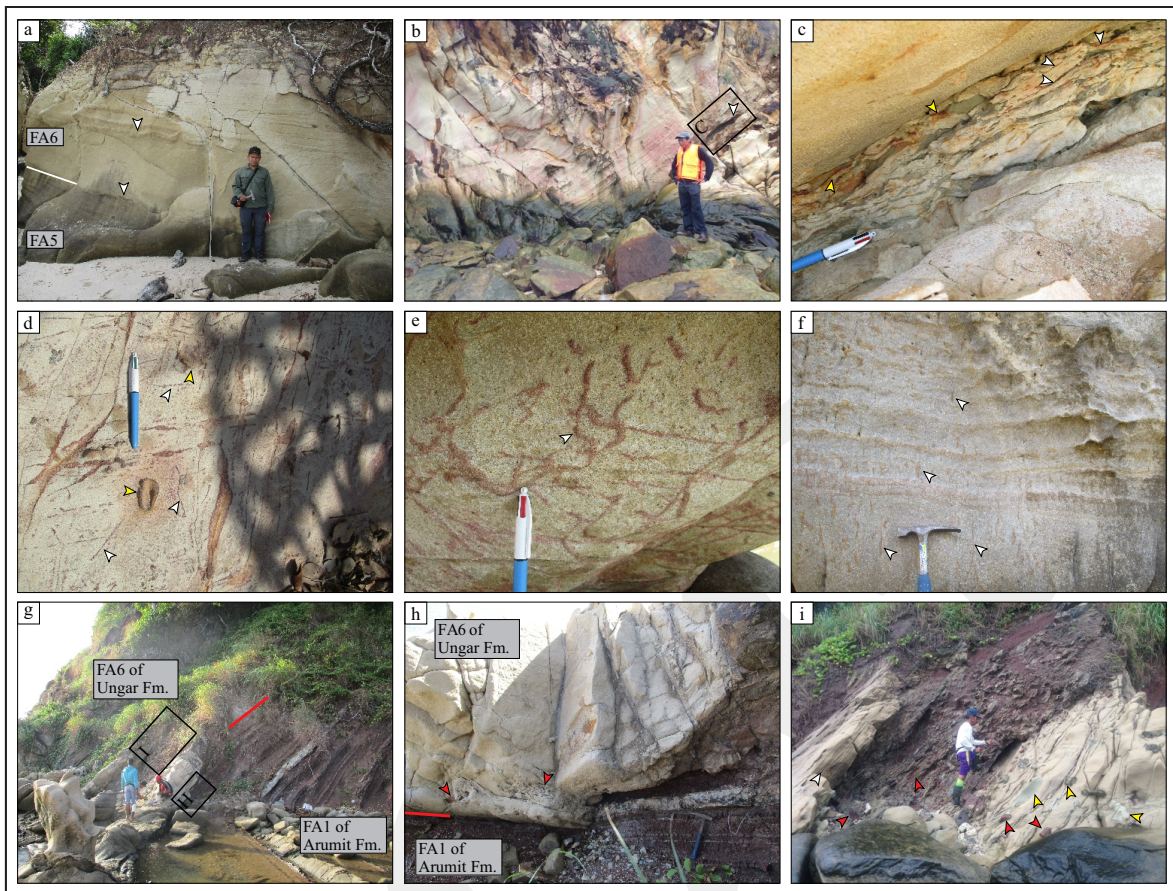


Figure 11. Field photographs of foreshore deposits (FA6) of Ungar Formation. Height of the man is 170 cm. Length of the pen and hammer is 14.5 cm and 33 cm respectively. a and b) Planar parallel bedding and low-angle stratified beds of fine-grained sandstone show scour surfaces (white arrows). White dash line: FA boundary. c) Scour surface in Figure 11b occupied by sandstone and mud lenses form flaser bedding. Iron oxide concretions (yellow arrows) are found within the scour surface. d and e) *Macaronichnus* trace-fossils (white arrows) are found in the bedding plane. Fe-mineralization present filled the burrow and in concretion form (yellow arrows). f) *Skolithos* (white arrows) trace-fossils in a planar bedded fine-grained sandstone. g and h) Erosional unconformity contact (red lines) between parallel bedded fine-grained sandstone (FA6 of Ungar Formation) and heterolithic bedding (FA1 of Arumit Formation) show mud clasts deposited above the erosional surface (red arrows). i) Matrix supported mud (red arrows) and lithic (yellow arrows) clasts overlain by parallel fine-grained sandstone intercalated with gravel layer containing scattered granule to pebble.

(Figure 6i) were observed in the siltstone interval. Micro HCS (Figure 6g), fluid mud layer, and rip up fluid mud clast are locally present at this FA.

Interpretation

Heterolithic bedding with flaser bedding at the base, wavy bedding at the middle, and lenticular bedding at the top in fining upward succession are considered to be originated in intertidal flat setting (Fan, 2013). A prograding intertidal flat will build up a fining-upward succession due to general seaward-coarsening trend of surface sediment on the accretional intertidal flats (Fan, 2013). Cyclical tidal rhythmites occurring at this

intertidal FA are considered to be equivalent to cyclic tidal bundle sequences in the subtidal channel settings (Fan, 2013). Single and double mud/carbonaceous drapes and organic debris marking on some planar laminated stratification suggest rhythmically fluctuating energies of tidal current (Vakarelov *et al.*, 2012). The occurrence of desiccation cracks supports the intertidal setting interpretation (Tucker and Wright, 1990; Lasemi *et al.*, 2012).

The presence of storm originated micro HCS structures indicates that the storm influence is able to reach the intertidal area. Tidal flats are lowered and sediment becomes sandier during

storm conditions resulting in deposition of sand dominated layers which may contain hummocky cross-stratification (Fan, 2013). Fluid mud occurring at this FA is relatively thinner than fluid mud at FA1. The mud layers are thin at the intertidal zone, because the suspended sediment concentration at the level of the intertidal zone is much less than that in channel bottom/subtidal zone (Dalrymple and Choi, 2007).

Facies association 3 (FA3): supratidal flat deposits

Description

The association at west Vulmali section is composed of reddish dark brown rooted mudstone bed to alternate between silty mudstone laminae and discontinuous lignite laminae (Figures 2 and 7a). Laminae sets at the top of mudstone bed are rhythmic, alternating between lignite laminae and silty mudstone (Figure 7b). The total thickness of this FA is 10 cm. At west Ungar section, this FA occurs as white cream coloured mudstone, undulatory surface with red, black, and orange Fe-mineralization (iron and manganese) filling in the cracks (Figures 3 and 7c - f). The unit thickness is 12 to 25 cm.

Interpretation

Sediment deposition on supratidal setting owes to flocculation of fine sediment in the water column (Christiansen *et al.*, 2000). Mudstone bed was deposited by this process with a longer term low energy depositional phase (Dashtgard and Gingras, 2005). The rhythmic laminae sets of this FA are considered as the products of rhythmically fluctuating tidal current energies. Modern salt-marsh deposits at the Waterside Marsh, Canada, show rhythmic laminae sets (Dashtgard and Gingras, 2005). Lignite laminae is interpreted to form within shallower bodies of standing water at small ponds with vegetated zone. Peaty organic residues were able to form with conditions of sufficient vegetation growth, reduced oxidation, and reduced clastics input (Fielding, 1987). The presence of root structure supports the vegetated condition.

Undulatory surface at the mudstone bedding represents the upper surface and is the primary depositional surface of the supratidal deposits (Dashtgard and Gingras, 2005). The crack structure showing triple junctions found at west Ungar section was interpreted as incomplete desiccation mudcracks. Incomplete mudcrack system consisting of short, though often intersecting cracks caused by desiccation has insufficient time to fully develop (Plummer and Gostin, 1981). The occurrence of desiccation mudcracks is indicators of exposure at a subaerial environment (Plummer and Gostin, 1981). Locally, Fe-mineralization filling in the cracks supports the supratidal zone interpretation (Gingras and MacEachern, 2012).

Palynological analysis conducted at lignite layer also supports the supratidal zone interpretation. The dominance of *Araucariacites*, *Callicialasporites*, and *Classopollis* which belong to a coastal plant community (Abbink *et al.*, 2004; Gedl and Ziaja, 2012) indicates that the lignite deposition was mainly influenced by seashore vegetation. Coastal plant communities include plant that grew just along the coast, never submerged by the sea but under a constant influence of salt spray (Abbink *et al.*, 2004; Gedl and Ziaja, 2012). The common occurrences of dinoflagellata cysts such as *Prolixosphaeridium parvispinum*, *Canningia reticulata*, *Oligosphaeridium diluculum*, and *Diacanthum hollisteri* suggest marine influenced condition during the deposition of the lignite layer. The minor presence of bisaccate pollen grain such as *Alisporites* and *Podocarpidites*, and monosulcate pollen grain such as *Cycadopites* indicates lowland and upland/highland areas were nearby (Abbink *et al.*, 2004; Gedl and Ziaja, 2012).

Ungar Formation

Facies association 2 (FA2): intertidal flat deposits

Description

FA2 of Ungar Formation exposed at west Vulmali section consists of 160 cm fining upward succession of dominant dark gray fine-grained sandstones to dominantly light

gray mudstone (Figure 2). It, vertically, shows changes from flaser bedding through wavy bedding, and to lenticular bedding (Figures 8a - c). Some mudstones and sandstones show rhythmic alternations both in the cross-bed and the planar laminae (Figures 8d - f). Cross-bedded occurring in fine-grained sandstones with mud drapes separate the cross-bed into tidal bundles (Figures 8a, b, d, and e). Single and double mud/carbonaceous drapes occur throughout the interval of this FA (Figures 8a - f). Intraclast pebble-sized breccia is presents in the mudstone dominant interval (Figures 8a - c). Intense desiccation cracks occur predominantly in the mudstone layers (Figures 8a - c). This FA contains root traces (Figures 8a and g) with locally minor synsedimentary fault (Figures 8f). At east Vulmali section, FA2 consists of yellowish brown very fine-grained sandstone and red mudstone (Figures 5, 8h, and i). The sandstone thickness is 50 cm and it contains current ripples with mud draped foresets. The mudstone of 10 cm thick contains light green fluid mud.

Interpretation

This FA is interpreted to be deposited by the same processes as intertidal deposit of Arumit Formation. The presence of vertical changes from flaser bedding, through wavy bedding and to lenticular bedding, tidal rhythmites, tidal bundles, the occurrence of single and double mud/carbonaceous drapes, desiccation cracks, and fluid mud are all the same main features with intertidal deposit of Arumit Formation. Desiccation cracks and brecciated beds suggest a periodical subaerial environment. The presence of root trace supports an intertidal depositional environment interpretation. Periodic exposure result in desiccation and mud cracks is typical for tidal flats, particularly in the upper intertidal and supratidal settings (Tucker and Wright, 1990; Lasemi *et al.*, 2012). Minor synsedimentary fault was produced by penecontemporaneous deformation resulting from a movement of muddy semiconsolidated sediment under the influence of gravity (Reineck and Singh, 1980; Boggs, 2011).

Facies association 4 (FA4): marine offshore to lower shoreface deposits

Description

This FA is dominated by parallel laminated yellowish, reddish, and light brown very fine-grained sandstones with a subordinate proportion of silty very fine-grained sandstones (Figures 2 - 4, and 9). The facies association thickness is up to 12 m. The less common ones are low-angle parallel stratification (Figures 9a and b) and undulatory lamination intervals (Figures 9c and e). Hummocky cross-stratified association presents at the top part of this FA (Figures 9d - g). Carbonaceous detritus concentration locally marks internal laminae within the sandstone layers (Figures 9c and e). Scattered granule to pebble clasts occur in stringers and isolated clusters (Figures 9c - f, h, and i). Mud clasts are common at the base of this FA (Figures 9j - l). Another less common sedimentary structure is flame structure (Figure 9k).

Interpretation

FA4 is interpreted as the marine offshore to lower shoreface deposits, here defined as being deposited below the fair-weather wave base (FWWB). Abundant sand character indicates that this FA was deposited during a progradation phase. Under the progradation condition, sand is likely to be far more abundant and can reach out onto the shelf (Clifton, 2006). Parallel laminated to low-angle laminated with sharp based throughout the interval suggests deposition during episodic waxing and waning currents, interpreted as related to storm-induced geostrophic flow (Clifton, 2006; Vakarelov *et al.*, 2012). Hummocky cross-stratification sandstones are interpreted as oscillatory dominant current deposits due to strong waves during storm events (Harms *et al.*, 1975; Dumas and Arnott, 2006). Hummocky cross-stratification sandstone is the characteristic of shallow marine storm-dominated inner shelf to lower shoreface deposits (Harms *et al.*, 1975; Johnson and Baldwin, 1996; Midtgaard, 1996). It forms near storm weather wave base, below and above fair weather wave base (Dumas and Arnott, 2006).

Carbonaceous detritus concentration marking the undulatory lamination is interpreted as representation of immediately post-storm (waning energy) sedimentation that was not completely eroded by subsequent storm-related scour (Vakarelov *et al.*, 2012). Scattered granules to pebbles in this FA are interpreted as reworked and remnant of post-storm lags (Clifton, 2006). Erosional surface overlain by mud clast at the base of this FA is interpreted as a transgressive lag at a transgressive erosion surface (Walker and Flint, 1992; Clifton, 2006; Suter, 2006). Flame structure was caused mainly by loading of water-saturated muddy layers which are less dense than overlying sands, and are consequently squeezed upward into the sand layers (Boggs, 2011).

Facies association 5 (FA5): upper shoreface deposits

Description

This FA mainly consists of yellowish, reddish, and light brown fine- to medium-grained sandstones, moderately well- to well-sorted (Figures 2 - 4). The facies association thickness is up to 5 m. Layers and lenses of granule sandstones and granule to pebble conglomerates commonly occurring show imbricated clasts. Uncommon very coarse-grained sandstone occur at MS 7. The sandstones have planar lamination and bedding (Figure 10a), low-angle cross-stratified (Figures 10a and h), trough and planar cross-bedding (Figures 10c - f and i - l) and wave ripple (Figure 10g). Cross-beds consist of sandstones, granule sandstones and granule to pebble conglomerates (Figure 10i - l). The less common sedimentary structure is convolute bedding (Figure 10h). FA5 overlays FA4 with both sharp based/erosional contact (Figures 10j and k) and transitional contact (Figure 10l). The erosional contact separates coarser, cross-bedded gravel sandstone from subjacent finer sandstone. Mud clasts are found above the erosional surface between FA5 and FA2 (Figure 8i).

Interpretation

FA5 is interpreted as the upper shoreface deposits, here defined as being deposited above the fair-weather wave base (FWWB). Planar

lamination and bedding are formed by bedload processes with settling of fines from suspension or traction of sand (Boggs, 2011). It is an upper flow regime flat-bed with high velocity current at shallow water depth (Collinson *et al.*, 2006). Low-angle cross-stratified deposits are interpreted to form by the combination of oscillatory flow and unidirectional current (Duke *et al.*, 1991). Trough and planar cross-bedding deposits are interpreted as 2D and 3D subaqueous dunes (Allen, 1963; Miall, 1977), formed mainly by longshore currents, and interpreted as deposits of the surf zone (Clifton, 2006). The wave ripples are interpreted as low energy oscillatory deposits (Clifton, 2006; Vieira and Scherer, 2017). Cross-bedded coarse sand and gravel are assumed to form in a pebbly to coarse sand texture dominant coast under dominant storm conditions (Clifton, 2006). Isolated layers and lenses of gravel interbedded with sand form where the nearshore is composed of gravel and two-dimensional ripples or megaripples predominate (Clifton, 2006). Intercalation of granule to pebble conglomerates shows imbricated clasts, with cross-bedded sand and gravel probably represent upper shoreface deposits (Babic and Zupanic, 1998; Clifton, 2006). Convolute bedding is an indication of high sediment supply (Reading and Collinson, 1996; Collinson *et al.*, 2006). The presence of this sedimentary structure at the upper shoreface settings with high sediment reworking suggests a representation of rare episodes of rapid deposition. Erosional surface at the base of upper shoreface deposits overlying FA4 was interpreted as a result of progradation in the bar-trough system (Clifton, 2006). The common presence of small pebbles in the FA5 sandstone below the contact suggests that the erosional surface does not represent a major break in facies succession (Clifton, 2006). Mud clast at the base above erosional surface is also interpreted as a transgressive lag, the same as transgressive lag of FA4.

Facies association 6 (FA6): foreshore deposits

Description

This facies association is composed of well- to moderately well-sorted, yellowish, reddish,

and light brown very fine- to medium-grained sandstones (Figures 2 - 4). The facies association thickness is up to 5 m. The sandstones are characterized by the planar parallel bedding and low-angle stratified beds (Figures 11a and b). Uncommon scarce scour surfaces that separate distinct foreshore packages are identified. The scour surface slot is occupied by the intercalation of fine-grained sandstone and mudstone lenses to form the flaser bedding (Figures 11b and c). These sandstones are occasionally bioturbated. Identified trace-fossil are *Macaronichnus* and *Skolithos* (Figures 11d - f). Locally, Fe-mineralization is found filling the burrow and in a concretion form (Figures 11b and c). Scattered granule to pebble and gravel lenses or layers intercalated with planar lamination sandstones are rarely present (Figures 9l and 11i). Mud clasts above erosional surface are also found in this FA at west Ungar section, occurring at the contact with Arunit Formation (Figures 11g and h). Above it there are matrix supported mud and lithic clast, poor-sorted and angular to moderate-rounded shape (Figure 11i). Mud and lithic clast found at this location are up to boulder size, 40 cm.

Interpretation

FA6 is interpreted as the foreshore deposit, here defined as being deposited between mean high water and mean low water. As the waves approaching the beach, it then passes through a breaker zone and ends as swash and backwash zone on the beach foreshore where the bed is planar, and the sediment contains gently inclined or planar parallel stratification (Clifton, 2006). Beach foreshores are eroded during storms, and deposits aggrade in fair-weather intervals (Clifton, 2006). Thus, intercalated planar parallel stratification and low-angle stratified beds are interpreted as the result of swash and backwash processes by breaking waves on the foreshore (McCubbin, 1982; Clifton, 2006). The scour surfaces are interpreted as a mark of the storm events that separate deposition of each package consisting planar parallel stratification and low-angle stratified beds that correspond to a period

of time of fairweather (Catuneanu, 2006). Deposition of flaser bedding is interpreted to correspond to immediately post-storm sedimentation (waning energy) which also suggested tide influence period at this wave-dominated FA deposition (Vakarelov *et al.*, 2012). The presence of *Macaronichnus* and *Skolithos* trace-fossils supports the foreshore interpretation (Pemberton *et al.*, 2001; Buatois *et al.*, 2016) as well as Fe-mineralization fills the burrow (Gingras and MacEachern, 2012). Scattered pebbles and gravel lenses or layers are interpreted as coarser grains that were left behind and trapped at the foreshore after the storm (Clifton, 2006). Mud clast at the base of FA6 and its contact with Arunit Formation are also interpreted as a transgressive lag, the same as transgressive lag of FA4 and FA5. Matrix supported mud and lithic clast with the clast size up to 40 cm are interpreted to be deposited from debris flows at rocky shore platforms with boulders from cliff collapses.

Age determination and stratigraphy

Two well preserved assemblages of radiolaria from two samples of dark brown chert/red and brown mudstones at Ungar Island, from the same section with Arunit Formation are present at this paper (MS 13), yielded an upper Valanginian to Barremian (Early Cretaceous) age, and an upper Tithonian (Late Jurassic) to Berriasian (Early Cretaceous) age. Jasin and Haile (1996) concluded that most probable age range of this unit which is located below massive yellowish-weathering sandstone, recognized as Ungar Formation in this paper, are from Berriasian to Barremian (Early Cretaceous) age.

Despite obtaining ten samples prepared for the palynological analysis, only one sample (lignite sample of FA3 Arunit Formation) contains enough palynomorph and dinoflagellata cysts to provide reliable results (Figure 12). Valuable palynomorph and dinoflagellata cyst taxa contained at this sample for age determination are *Ruffordiaspora australiensis* (Cookson, 1953; Dettmann and Clifford, 1992), *Biretisporites eneabbaensis* (Backhouse, 1988), and *Canningia*

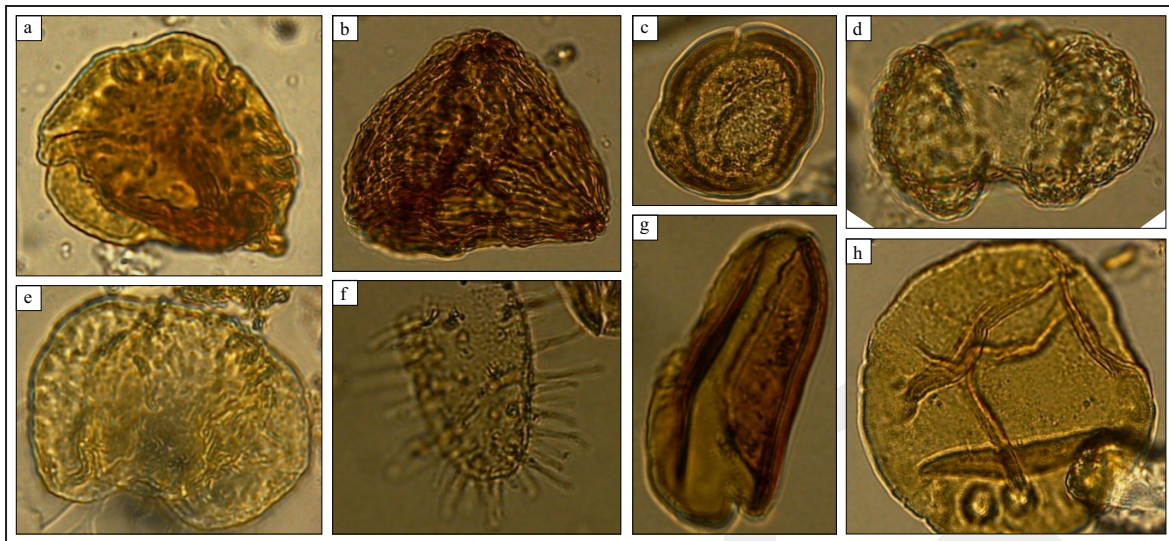


Figure 12. Photomicrographs of selected palynomorphs taxa of lignite layer of the Arumit Formation. Photographed at a magnification of x1000. a) *Callialasporites dampieri* (Balme, 1957) Dev, 1961 . b) *Ruffordiaspora australiensis* (Cookson, 1953) Dettmann and Clifford, 1992. c) *Classopollis torosus* (Reissinger, 1950) Couper, 1958 emend. Burger, 1965. d) *Podocarpidites* sp. e) *Alisporites* sp. f) *Prolixosphaeridium* sp. g) *Cycadopites* sp. h) *Araucariacites australis* Cookson, 1947.

reticulata (Cookson and Eisenack, 1960). The first appearance of *Ruffordiaspora australiensis* and *Biretisporites eneabbaensis* is at the base of Berriasian. While the last appearance of *Canninia reticulata* is at Barremian (Helby *et al.*, 1987) which suggests probable Berriasian to Barremian age range for the sampled strata.

The stratigraphic position of Ungar Formation located above Arumit Formation ensures that Ungar Formation is younger than Barremian (Figures 2 and 3). Clasts of red and green mudstones, siltstone, and sandstone of Arumit Formation found as fragments in Ungar Formation and erosional contact between these two units provide facts of subaerial exposure and erosion of Arumit Formation into the deposition of Ungar Formation (Figures 9j and 11g - i). Ungar Formation presented at this paper is assigned as the Cretaceous Ungar Formation (Zimmermann and Hall, 2014) or the upper part of the Ungar Formation (Charlton, 2012). The zircon U-Pb analysis shows that the youngest grain of the Cretaceous Ungar Formation is Upper Cretaceous, 83.7 Ma (Zimmermann and Hall, 2014). Therefore, probable age range suggestion for Ungar Formation at the studied area is Aptian to Santonian (Early to Late Cretaceous). Previously named as the Arumit Member of Un-

gar Formation (Charlton in Jasin and Haile, 1996; Charlton, 2012) is proposed in this paper as Arumit Formation with distinct lithological characteristic and age as described above. The type locality is proposed in west Ungar Island section (Figure 3).

Depositional Model

Based on the above-mentioned facies association analysis, a progradational open-coast tidal flat depositional environment is suggested for the deposition of the Arumit Formation at the studied area (Figure 13). Progradational open-coast tidal flat successions consist of two parts, with the lower half coarsening upward from lower to upper subtidal flats (FA1), and the upper half fining upward from lower to upper intertidal flats (FA2) to supratidal (FA3) (Li *et al.*, 1992 in Fan, 2013; Fan, 2012, 2013).

Sediments of the Arumit Formation are furthermore able to be divided into sandy open-coast tidal flats and muddy open-coast tidal flats, based on the presence of HCS and sand or mud domination in the succession. Typical HCS can be common in the sandy open-coast tidal flat deposits, but is not present in muddy open-coast tidal flat deposits (Fan, 2012). Vertical succession of Arumit Formation at west Vulmali section

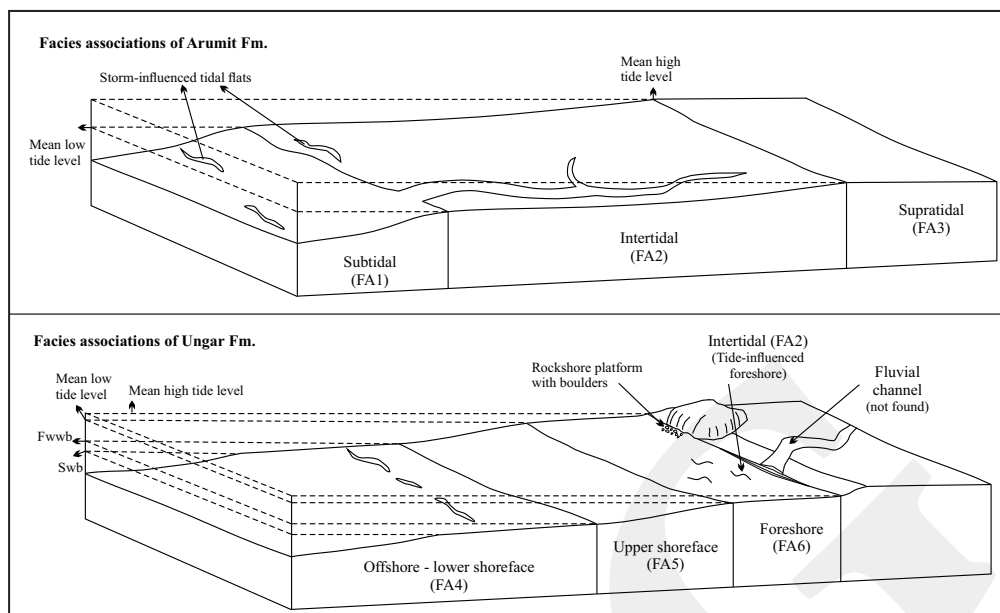


Figure 13. Depositional model and facies associations of Arumit and Ungar Formation. Abbreviation = Fwwb: fair weather wave base and Swb: storm wave base.

(MS 1; Figure 2) is interpreted to be deposited in a sandy open-coast tidal flat shown by the occurrences of HCS and domination of sandy sediment. It is different with the sediments of the Arumit Formation at west Ungar section (MS 12 and MS 13; Figure 3) which is interpreted to be deposited in muddy open-coast tidal flat settings with the rare presence of HCS and domination of mud in the succession. Tidal channel networks generally not much developed or event are absent on the open-coast tidal flats (Fan, 2012). Identified tidal channel facies as described in FA1 is present in the muddy open-coast tidal flat part (MS 12 and MS 13; Figure 3). Fluid mud is present predominantly in the sandy open-coast tidal flat part (MS 1; Figure 2).

The presence of tidal rhythmites, mud drapes, and fluid mud in sediments of Arumit Formation are diagnostic features of tide domination process in the deposition of this unit (Boyd *et al.*, 2006; Longhitano *et al.*, 2012; Fan, 2013). The occurrence of deep water originated radiolaria described by Jasin and Haile (1996) preserved in Arumit Formation is interpreted as the result of upwelling process. Upwelling is a process in which deep, cold water rises toward the surface. The winds blow across the ocean surface pushing

water away, then surface water is replaced by cold nutrient-rich water that “wells up” from below (Anonymous, 2018). Radiolarian fossils occur in a facies representing an extremely wide range of depositional depth. These organisms as with other pelagic faunas may occur in shallow water deposits (Wever and Baudin, 1996).

Based on the sedimentary facies association described and interpreted above, an open-coast wave dominated depositional environment is proposed for the deposition of Ungar Formation in the studied area (Figure 13). Progradation shoreline successions dominate in three studied sections shown by the domination of shallowing upward pattern. Transgressive phases only occurred in the middle part of west and east Vulmali section (FA2 in MS 6 and MS 14; Figures 2 and 3), marked by the presence of tidal deposits within shoreface deposits. This transgression phase occurred when base-level rise was higher than the rate of sedimentation (Clifton, 2006).

Parameters of open-coast settings that can influence the lithologies and stratigraphic succession of the deposit are: sand supply, texture, ambient energy, morphology, dominant conditions, and base level (Clifton, 2006). Sand supply was abundant during the deposition of shoreline

deposits of the Ungar Formation characterized by the relatively absent of mud and domination of sand. Even though fluvial deposit is not present in the studied section, abundant sand condition in the entire Ungar Formation section suggests that there was a fluvial feeder that supplies abundant sand to the shoreline area. Detrital modes suggest a recycled orogen to continental block origin of the Cretaceous Ungar Formation (Zimmermann and Hall, 2014). They also indicate this sandstone as a reworking of Triassic and Jurassic formations, plus additional Cretaceous and also Jurassic populations that suggest an Asian rather than Australian origin. Coarse sand to pebbly texture condition is present in the middle part of west Vulmali section (MS 5, MS 7 and MS 8; Figure 2), Ungar section (MS 12 and MS 13; Figure 3), and at the upper part of east Vulmali section (MS 14; Figure 4), characterized by cross-bedded, layer, and lenses of sand and gravel. Fine sand texture condition is present at the lower and upper parts of west Vulmali section (MS 1-MS 4 and MS 9-MS 11; Figure 2) and the lower part of east Vulmali section (MS 14; Figure 4). Low

to moderate energy setting dominates the entire wave dominated sediments of the Ungar Formation at the three studied sections, characterized by relatively thin of FA6 with the thickness varying between 1,4 to 3 m. High energy coast only occurred at the upper part of west Vulmali section where FA6 is relatively thick, 4 to 5 m (MS 9 and MS 10; Figure 2).

Early to Late Cretaceous Palaeogeography Implications

The extensional phase with NE-SW trends commenced in Triassic through Jurassic to Early Cretaceous resulted in rifting and continental breakup of the NW Shelf (Barber *et al.*, 2003). Following the Mesozoic rifting, a microcontinental terrane was detached from the western margin of the Australian Continent (Charlton, 2012). This microcontinental terrane in the Tanimbar area was becoming the sediment source for the Early to Late Cretaceous sediments (Arumit and Ungar Formations) which were deposited in shallow marine environments (Figure 14). Different with Tanimbar area, the

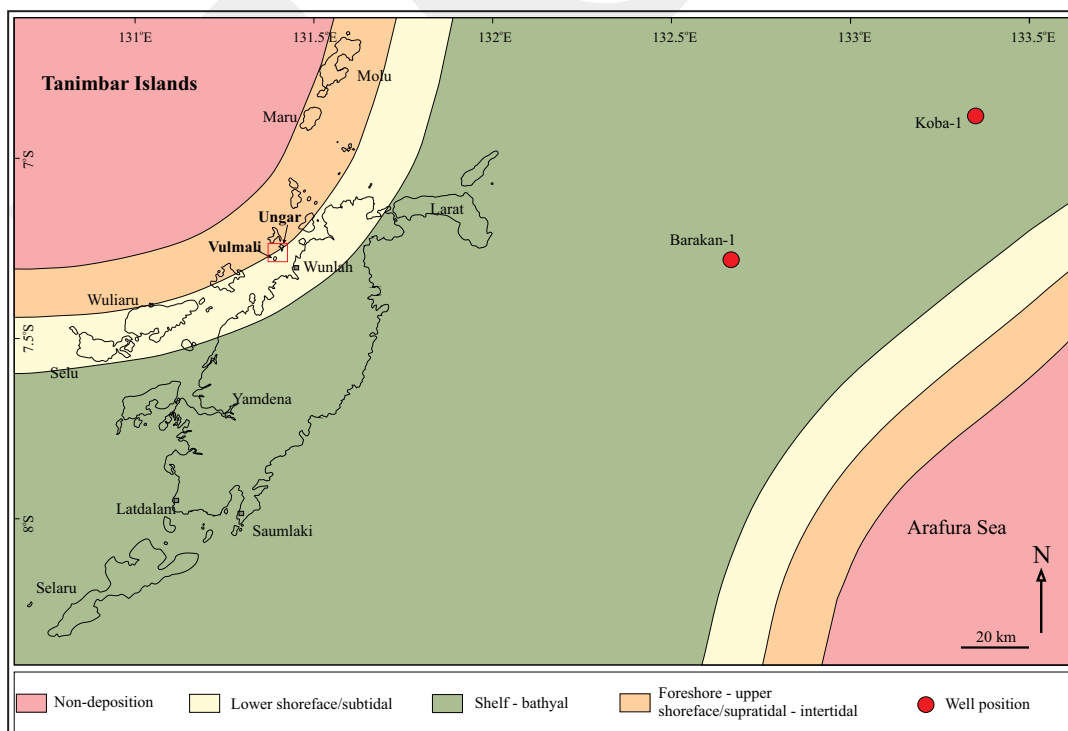


Figure 14. Cretaceous palaeogeography of Tanimbar Islands and Arafura Sea, adapted from Barber *et al.* (2003) and Charlton (2012).

Arafura Sea area was situated in the margin of the Australian Continent (Barber *et al.*, 2003). The sediments of Early to Late Cretaceous of Koba-1 and Barakan-1 wells were deposited in outer neritic to bathyal environments (Promet, 1984; Union Texas, 1995), in a basinward position between the microcontinental terrane at the west and Australian Continent at the east.

CONCLUSIONS

- Early Cretaceous Arumit Formation comprises three facies associations: subtidal, intertidal, and supratidal deposits. A progradational open-coast tidal flat depositional environment is suggested for the deposition of sediments of the Arumit Formation.
- Early to Late Cretaceous Ungar Formation in the studied area consist of four facies associations: intertidal, marine offshore to lower shoreface, upper shoreface, and foreshore deposits. An open-coast wave dominated depositional environment is proposed for the deposition of sediments of the Ungar Formation.

ACKNOWLEDGEMENT

The study was undertaken with financial and laboratory facility supports from The Centre for Geological Survey, Geological Agency, Ministry of Energy and Mineral Resources of Indonesia. The author is grateful to Ryan Akbar Fadhilah, Muhammad Nurhidayat, and Herwinsyah for their assistances during the field work. The author is indebted to Ani Khrisnawati and Sumarjadi for their assistances during the laboratory process. This paper greatly benefits from constructive reviews of anonymous reviewers.

REFERENCES

- Abbink, O.A., Van Konijnenburg-Van Cittert, J.H.A., and Visscher, H., 2004. A sporomorph ecogroup model for the Northwest European Jurassic-Early Cretaceous: concepts and framework. *Netherlands Journal of Geosciences, Geologie en Mijnbouw*, 83, p.17-38. DOI: 10.1017/S0016774600020436.
- Allen, J.R.L., 1963. The classification of cross-stratified units, with notes on their origin. *Sedimentology*, 2 (2), p.93-114. DOI: 10.1111/j.1365-3091.1963.tb01204.x.
- Anonymous, 2018. What is upwelling? <https://oceanservice.noaa.gov/facts/upwelling.html> [28 June 2018].
- Ashley, G.M., 1990. Classification of large-scale subaqueous bedforms: a new look at an old problem. *Journal of Sedimentary Petrology*, 60 (1), p.160-172. DOI: 10.2110/jsr.60.160.
- Babić, L. and Zupanić, J., 1998. Nearshore Deposits in the Middle Eocene Clastic Succession in Northern Dalmatia (Dinarides, Croatia). *Geologia Croatica*, 51 (2), p.175-193. DOI: 10.4154/GC.1998.14
- Barber, P., Carter, P., Fraser, T., Baillie, P., and Myers, K., 2003. Paleozoic and Mesozoic petroleum systems in the Timor and Arafura seas, eastern Indonesia. *Proceedings of Indonesian Petroleum Association, 29th Annual Convention and Exhibition*, Jakarta.
- Boggs, S., 2011. *Principles of sedimentology and stratigraphy*. Fifth Edition. Pearson Prentice Hall, 585pp.
- Boyd, R., Dalrymple, R.W., and Zaitlin, B.A., 2006. Estuarine and incised-valley facies models. In: Posamentier, H.W. and Walker, R.G. (eds.), *Facies Models Revisited. SEPM Special Publication*, 84, p.171-235. DOI: 10.2110/pec.06.84.0171
- Buatois, L.A., Carmona, N.B., Curran, H.A., Netto, R.G., Mángano, M.G., and Wetzel, A., 2016. The Mesozoic Marine Revolution. In: Mángano M. and Buatois, L. (eds.) *The Trace-Fossil Record of Major Evolutionary Events. Topics in Geobiology*, vol 40. Springer, Dordrecht, p.19-134. DOI: 10.1007/978-94-017-9597-5_2
- Catuneanu, O., 2006. *Principles of Sequence Stratigraphy*. Elsevier Science, 386pp.

- Charlton, T.R., de Smet, M.E.M., Samodra, H., and Kaye, S.J., 1991. The stratigraphic and structural evolution of the Tanimbar Islands, eastern Indonesia. *Journal of Southeast Asian Earth Sciences*, 6, (3/4), p.343-358.
- Charlton, T., 2012. Permian-Jurassic Palaeogeography of the SE Banda Arc Region. *Berita Sedimentologi - Indonesian Journal of Sedimentary Geology*, 24, (7), p.5-17.
- Charlton, T., 2018. The Petroleum Potential of the Tanimbar islands. <https://www.manson.demon.co.uk/tanimbar.html> [28 June 2018].
- Choi, K.S., Dalrymple, R.W., Chun, S.S., and Kim, S.P., 2004. Sedimentology of modern, inclined heterolithic stratification (IHS) in the macrotidal Han River delta, Korea. *Journal of Sedimentary Research*, 74 (5), p.677-689. DOI: 10.1306/030804740677.
- Christiansen, T., Wiberg, P.L., and Milligan, T.G., 2000. Flow and Sediment Transport on a Tidal Salt Marsh Surface. *Estuarine, Coastal and Shelf Science*, 50 (3), p.315-331. DOI:10.1006/ecss.2000.0548
- Clifton, H.E., 2006. A reexamination of facies models for clastic shorelines. In: Posamentier, H.W. and Walker, R.G. (eds), *Facies Models Revisited. SEPM Special Publication*, 84, p.293-338. DOI: 10.2110/pec.06.84.0293
- Collinson, J.D., Mountney, N., and Thompson, D., 2006. *Sedimentary Structures*. Third edition, Terra, Harpenden, Hart, 292pp.
- Dalrymple, R.W., 2010. Tidal depositional systems. In: James, N.P. and Dalrymple, R.W. (eds.), *Facies Models 4. Geological Association of Canada*, St. John's, pp.201-231.
- Dalrymple, R.W. and Choi, K., 2007. Morphologic and facies trends through the fluvial-marine transition in tide-dominated depositional systems: A schematic framework for environmental and sequence-stratigraphic interpretation. *Earth-Science Reviews*, 81, p.135-174. DOI: 10.1016/j.earscirev.2006.10.002
- Dashtgard, S.E. and Gingras, M.K., 2005. Facies architecture and ichnology of recent salt-marsh deposits: Waterside Marsh, New Brunswick, Canada. *Journal of Sedimentary Research*, 75 (4), p.596-607. DOI: 10.2110/jsr.2005.049
- Davis, R.A., 2012. Tidal signatures and their preservation potential in stratigraphic sequences. In: Davis, R.A. and Dalrymple, R.W. (eds.), *Principles of tidal sedimentology*. Springer, Dordrecht, p.35-55. DOI: 10.1007/978-94-007-0123-6_3
- Duke, W.L., Arnott, R.W.C., and Cheel, R.J., 1991. Shelf sandstones and hummocky cross-stratification: New insights on a stormy debate. *Geology*, 19 (6), p.625-628. DOI: 10.1130/0091-7613(1991)019<0625:SSAHCS>2.3.CO;2
- Dumas, S. and Arnott, R.W.C., 2006. Origin of hummocky and swaley cross-stratification - The controlling influence of unidirectional current strength and aggradation rate. *Geology*, 34 (12), p.1073-1076. DOI: 10.1130/G22930A.1
- Faas, R.W., 1991. Rheological boundaries of mud. Where are the limits?. *Geo-Marine Letters*, 11 (3-4), p.143-146. DOI: 10.1007/BF02431000
- Fan, D., 2012. Open-Coast Tidal Flats. In: Davis, R.A. and Dalrymple, R.W. (eds.), *Principles of tidal sedimentology*. Springer, Dordrecht, p.187-229. DOI: 10.1007/978-94-007-0123-6_9
- Fan, D., 2013. Classifications, sedimentary features and facies associations of tidal flats. *Journal of Palaeogeography*, 2 (1), p.66-80. DOI: 10.3724/SP.J.1261.2013.00018.
- Fielding, C.R., 1987. Coal depositional models for deltaic and alluvial plain sequences. *Geology*, 15 (7), p.661-664. DOI: 10.1130/0091-7613(1987)15<661:CDMFDA>2.0.CO;2
- Gedl, P. and Ziąja, J., 2012. Palynofacies from Bathonian (Middle Jurassic) ore-bearing clays at Gnaszyn, Kraków-Silesia Homocline, Poland, with special emphasis on sporomorph eco-groups. *Acta Geologica Polonica*, 62 (3), p.325-349. DOI: 10.2478/v10263-012-0018-7
- Gingras, M.K. and MacEachern, J.A., 2012. Tidal ichnology of shallow-water clastic settings. In: Davis, R.A. and Dalrymple, R.W. (eds.), *Principles of tidal sedimentology*. Springer,

- Dordrecht, p.57-77. DOI: 10.1007/978-94-007-0123-6_4.
- Harms, J.C., Southard, J.B., Spearing, D.R., and Walker, R.G., 1975. Depositional Environments as Interpreted From Primary Sedimentary Structures and Stratification Sequences. *SEPM Short Course 2*, 161pp. DOI: 10.2110/scn.75.02
- Helby, R., Morgan, R., and Partridge, A.D., 1987. A palynological zonation of the Australian Mesozoic. In: Jell, P.A. (ed.), *Studies in Australian Mesozoic Palynology. Memoir of the Association Australasian Palaeontologists*, 4, p.1-94.
- Ichaso, A.A. and Dalrymple, R.W., 2009. Tide- and wave-generated fluid mud deposits in the Tilje Formation (Jurassic), offshore Norway. *Geology*, 37 (6), p.539-542. DOI: 10.1130/G25481A.1
- Jasin, B. and Haile, N., 1996. Uppermost Jurassic-Early Cretaceous radiolarian chert from the Tanimbar Islands (Banda Arc), Indonesia. *Journal of SE Asian Earth Sciences*, 14 (1/2), p.91-100.
- Johnson, H.D. and Baldwin, C.T., 1996. *Shallow clastic seas*. In: Reading, H.G. (ed.), *Sedimentary environments: processes, facies and stratigraphy*. Third edition. Blackwell Science Oxford, p.232-280.
- Kaye, S. J., 1989. The structure of Eastern Indonesia: an approach via gravity and other geophysical methods. *Doctoral thesis*, Department of Geological Sciences, University of London. 240pp.
- Kirby, R. and Parker, W.R., 1983, Distribution and behavior of fine sediment in the Severn Estuary and inner Bristol Channel, U.K.. *Canadian Journal of Fisheries and Aquatic Sciences*, 40 (S1), p.83-95. DOI: 10.1139/f83-271
- Lasemi, Y., Jahani, D., Amin-Rasouli, H., and Lasemi, Z., 2012. Ancient Carbonate Tidalites. In: Davis, R.A and Dalrymple, R.W. (eds.). *Principles of tidal sedimentology*. Springer, Dordrecht, p.567-607. DOI: 10.1007/978-94-007-0123-6_21
- Li, S., Li, S., Shan, X., Gong, C., and Yu, X., 2017. Classification, formation, and transport mechanisms of mud clasts. *International Geology Review*, 59 (12), p.1-12. DOI: 10.1080/00206814.2017.1287014
- Longhitano, S.G., Mellere, D., Steel, R.J., and Ainsworth, R.B., 2012. Tidal depositional systems in the rock record: A review and new insights. In: Longhitano, S.G., Mellere, D., and Ainsworth, R.B. (eds.), *Modern and ancient depositional systems: perspectives, models and signatures. Sedimentary Geology*, Special Issue, 279, p.2-22. DOI:10.1016/j.sedgeo.2012.03.024
- McCubbin, D.G., 1982. Barrier-island and strand-plain facies. In: Scholle, P.A. and Spearing D.R. (eds.), *Sandstone Depositional Environments. AAPG Memoirs*, 31, p.247-280. DOI: 10.1306/M31424C10
- Miall, A.D., 1977. A review of the braided-river depositional environment. *Earth-Science Reviews*, 13 (1), p.1-62. DOI: 10.1016/0012-8252(77)90055-1
- Midtgaard, H.H., 1996. Inner-shelf to lower-shelf hummocky sandstone bodies with evidence for geostrophic influenced combined flow, Early Cretaceous, West Greenland. *Journal of Sedimentary Research*, 66 (2), p.343-353. DOI: 10.1306/D4268342-2B26-11D7- 8648000102C1865D
- Mossop, G.D. and Flach, P.D., 1983. Deep channel sedimentation in the Early Cretaceous McMurray Formation, Athabasca Oil Sands, Alberta. *Sedimentology*, 30 (4), p.493-509. DOI:10.1111/j.1365-3091.1983.tb00688.x
- Pemberton, S.G., Spila, M., Pulham, A.J., Saunders, T., MacEachern, J.A., Robbins, D., and Sinclair, I.K., 2001. Ichnology and sedimentology of shallow to marginal marine systems: Ben Nevis and Avalon reservoirs, Jeanne d'Arc Basin. *Geological Association of Canada, Short Course Notes*, 15, 343pp.
- Plummer, P.S. and Gostin, V.A., 1981. Shrinkage cracks: desiccation or syneresis?. *Journal of Sedimentary Research*, 51 (4), p.1147-1156. DOI: 10.1306/212F7E4B-2B24-11D7-8648000102C1865D

- Promet, 1984. Koba-1 well completion report (unpublished).
- Reading, H.G. and Collinson, J.D., 1996. Clastic Coasts. *In: Reading, H.G. (ed.), Sedimentary Environments: Process, Facies and Stratigraphy*. Blackwells, Cornwall, p.154-231.
- Reineck, H.E. and Singh, I.B., 1980. *Depositional Sedimentary Environments*. Second Edition, Springer-Verlag Berlin Heidelberg, 551pp. DOI: 10.1007/978-3-642-81498-3.
- Sukardi and Sutrisno, 1989. *Geological Map of the Tanimbar Islands Quadrangle, Maluku. 1:250.000*. Geological Research and Development Centre, Bandung.
- Suter, J.R., 2006. Facies models revisited: clastic shelves. *In: Posamentier, H.W. and Walker, R.G. (eds.), Facies Models Revisited. SEPM Special Publication*, 84, p.339-397. DOI: 10.2110/pec.06.84.0339
- Tucker, M.E. and Wright, V.P., 1990. *Carbonate Sedimentology*. Blackwell Scientific Ltd, Oxford, 482pp. DOI: 10.1002/9781444314175
- Union Texas, 1995. Barakan-1 well completion report (unpublished).
- Vakarelov, K.B., Ainsworth, R.B., and MacEachern, J.A., 2012. Recognition of wave-dominated, tide-influenced shoreline systems in the rock record: Variations from a microtidal shoreline model. *In: Longhitano, S.G., Mellere, D., and Ainsworth, R.B. (eds.), Modern and ancient depositional systems: perspectives, models and signatures. Sedimentary Geology, Special Issue*, 279, p.23-41. DOI: 10.1016/j.sedgeo.2011.03.004
- Vieira, L.V. and Scherer, C.M.S., 2017. Facies architecture and high resolution sequence stratigraphy of an aeolian, fluvial and shallow marine system in the Pennsylvanian Piauí Formation, Parnaíba Basin, Brazil. *Journal of South American Earth Sciences*, 76, p.238-256. DOI: 10.1016/j.jsames.2017.03.009
- Walker, R.G. and Plint, A.G., 1992. Wave- and storm-dominated shallow marine systems. *In: Walker, R.G. and James, N.P. (eds.), Facies Models: Response to Sea-Level Change. Geological Association of Canada, Newfoundland*, p.219-238.
- Walker, R.G., 2006. Facies models revisited: Introduction. *In: Posamentier, H.W. and Walker, R.G. (eds.), Facies Models Revisited. SEPM Special Publication*, 84, p.293-338. DOI: 10.2110/pec.06.84.0001.
- Wever, P.D. and Baudin, F., 1996. Palaeogeography of radiolarites and organic-rich deposits in Mesozoic Tethys. *Geologische Rundschau*, 85 (2), p.310-326. DOI: 10.1007/BF02422237
- White, W.A., 1961. Colloid phenomena in sedimentation of argillaceous rocks. *Journal of Sedimentary Petrology*, 31 (4), p.560-570. DOI: 10.1306/74D70BE6-2B21-11D7-8648000102C1865D
- Zimmermann, S. and Hall, R., 2014. Provenance of Mesozoic Sandstones in The Banda Arc, Indonesia. *Proceedings of Indonesian Petroleum Association, 38th Annual Convention and Exhibition*, Jakarta.